Rydberg Excitons in novel two-dimensional materials: TMDCs and Xenes

Anastasia Spiridonova[1,2] and R. Ya. Kezerashvili[1,2]

[1]Departament of Physics, New York City College of Technology, Brooklyn, NY 11201

[2]Physics Program, The Graduate Center of CUNY, New York, NY 10016

Abstract

We study direct and indirect magnetoexcitons in novel two-dimensional materials such as transition-metal dichalcogenides (TMDCs) and Xenes, which are encapsulated or spatially separated by *h*-BN monolayers. The formation of magnetoexcitons in TMDC monolayer or heterostructure occur in the presence of the magnetic field which is perpendicular to the layer. The formation of magnetoexcitons in Xenes monolayer and heterostructure are studied in presence of both perpendicular magnetic and electric fields. We calculate the binding energies, energy contributions, and diamagnetic coefficients based on numerical solution of the Schrödinger equation using both the Rytova-Keldysh and Coulomb potentials for the description of electron-hole interaction. We find that the binding energies of magnetoexcitons in TMDCs can be tuned by the magnetic field. It is demonstrated that the binding energies of the magnetoexcitons of the Rydberg 1*s*, 2*s*, 3*s*, and 4*s* states in the Xenes monolayer and heterostructure could be tuned by changing both the external magnetic and electric fields. The calculations of the binding energies of magnetoexcitons and diamagnetic coefficients in TMDC heterostructures and Xenes monolayers and heterostructure are reported for the first time.

Theoretical Formalism

We examine Rydberg states of direct *A* magnetoexcitons in monolayers and indirect magnetoexcitons in double-layer heterostructures in parallel electric and magnetic fields perpendicular to the monolayer. We examine TMDCs: WSe_2, WS_2, $MoSe_2$, and MoS_2, monolayers encapsulated by *h*-BN, and Xenes[1]: silicene, stanene, germanene, free standing and *h*-BN encapsulated monolayers and *h*-BN heterostructures. The Hamiltonian for two-body system ($\hbar = c = 1$) [2]:

$$H = \frac{1}{2m_e}(-i\boldsymbol{\nabla}_e + e\boldsymbol{A}_e)^2 + \frac{1}{2m_e}(-i\boldsymbol{\nabla}_e - e\boldsymbol{A}_e)^2 + V(\boldsymbol{r}). \quad (1)$$

For direct excitons, the Rytova-Keldysh (RK) potential[3,4] (eq.2) was used. For indirect excitons, the RK (eq. 3) and Coulomb (eq. 4) potentials were used to demonstrate the importance of screening in heterostructures:

$$V_{RK}(\boldsymbol{r}) = -\frac{\pi k e^2}{2\kappa\rho_0}\left[H_0(\rho/\rho_0) - Y_0(\rho/\rho_0)\right], \quad (2)$$

$$V_{RK}(\boldsymbol{r}) = -\frac{\pi k e^2}{2\kappa\rho_0}\left[H_0\left(\sqrt{\rho^2+D^2}/\rho_0\right) - Y_0\left(\sqrt{\rho^2+D^2}/\rho_0\right)\right], \quad (3)$$

$$V_C\left(\sqrt{\rho^2+D^2}\right) = -\frac{ke^2}{\kappa\left(\sqrt{\rho^2+D^2}\right)} \quad (4)$$

Where $\sqrt{\rho^2+D^2} = \sqrt{\rho^2+(Nl_{h-BN})^2}$ see Fig. 3 for explanation.

Theoretical Formalism

To find the energy contribution to the binding energies from electric and magnetic fields, we implement code used implemented in [5]. The code numerically solves for eigenfunction and eigenvalues of Schrödinger equation for the relative motion of the electron and hole that is obtained by following [6]-[9]:

$$\left(-\frac{1}{2\mu}\nabla^2 + \frac{e^2}{8\mu}(\boldsymbol{B}\times\boldsymbol{r})^2 + V(\boldsymbol{r})\right)\psi(\boldsymbol{r}) = \mathscr{E}\psi(\boldsymbol{r}). \quad (5)$$

When the contribution to the binding energy from the electric and magnetic fields is small compared to the binding energy, the magnetoexciton binding energy can be expanded in Taylor[10] series. The energy contribution from the magnetic field to the binding energy is then found as:

$\Delta\mathscr{E} = \mathscr{E}_0 - \mathscr{E}(B,E)$. The diamagnetic coefficient is defined as: $\Delta\mathscr{E} = \sigma B^2$.

TMDCs

We used parameters that give the highest and lowest binding energies of *A* magnetoexcitons from [5] and [11], respectively. We calculate $\mathscr{E}_{A_{high/low}}$ for direct and indirect magnetoexcitons in TMDCs monolayer and double-layer heterostructures for magnetic field in the range from 0 to 30 T. For indirect magnetoexcitons, we vary the number of *h*-BN layers, *N*, that separate two monolayers from 1 to 6.

We examine TMDCs: WSe_2, WS_2, $MoSe_2$, and MoS_2, monolayers encapsulated by *h*-BN, and heterostructures, X-*h*-BN-X.

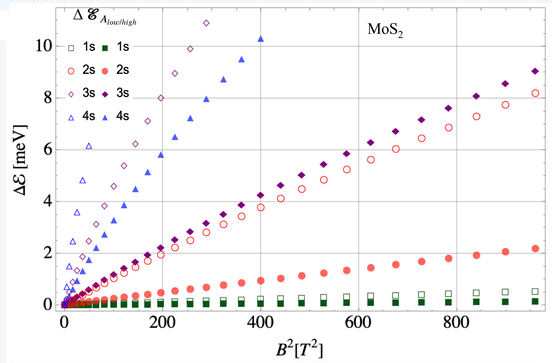

Fig. 1: Calculated change in $\Delta\mathscr{E}$ versus B^2 for states 1s-4s. $\Delta\mathscr{E}_{A_{low/high}}$ are calculated using parameters [5], [11] that highest and lowest $\mathscr{E}$. The calculations are performed for direct magnetoexcitons in MoS_2. Results are reported in [12].

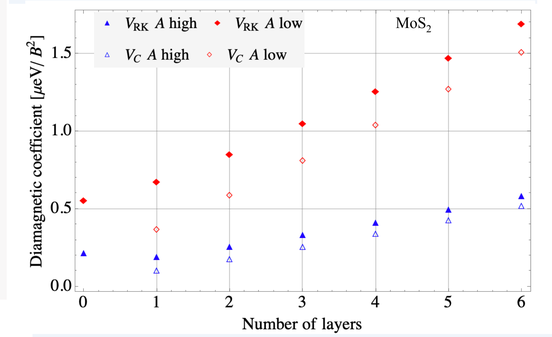

Fig. 2: The diamagnetic coefficients for MoS_2 for direct (*N*=0) and indirect magnetoexcitons (*N*=1-6). For indirect magnetoexcitons σ is extracted from $\mathscr{E}$ calculated using V_{RK} and V_C.

Xenes

We study Rydberg states of magnetoexcitons in Xenes: silicene, germanene, and stanene, in parallel electric and magnetic fields that are perpendicular to the monolayer. We study direct *A* magnetoexcitons in freestanding Xenes (FS, where vacuum is on both sides of the monolayer), see Fig. 3*a*, direct magnetoexcitons in Si monolayer encapsulated by *h*-BN (Si types I and II), see Fig. 3*b,* and indirect magnetoexcitons in double-layer heterostructure of FS Si and Si type I where two layers of Xene monolayers by *N* of *h*-BN, see Fig. 3*c*. We used the parameters given in [13]-[16]:

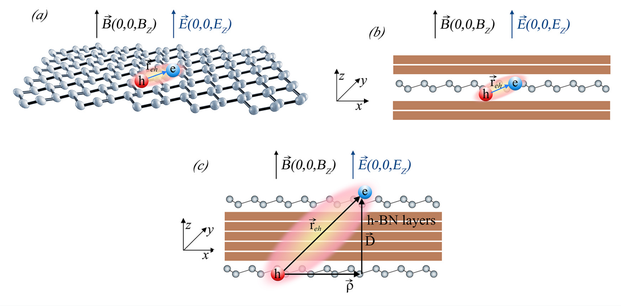

Fig. 3: Schematics for magnetoexcitons in Xenes monolayer and heterostructure. (a) A direct magnetoexciton in the freestanding buckled honeycomb lattice structure of silicene monolayer. (b) A magnetoexciton in silicene encapsulated monolayer. (c) An indirect magnetoexciton in silicene heterostructure. Adopted from [17].

In the external perpendicular electric field, the buckled structure of the Xene monolayers leads to appearance of potential difference between sublattices allowing to tune electron and hole masses. Masses of electrons and holes are equal in Xenes. Mass is found by[13,18]:

$$m = \frac{|\xi\sigma\Delta_{SO} - ed_0E|}{v_F^2} \quad (8)$$

Where $\xi, \sigma = \pm 1$ are the valley and spin indices, respectively, d_0 is the buckling constant, $2\Delta_{SO}$ is the intrinsic band gap, E is the electric field.

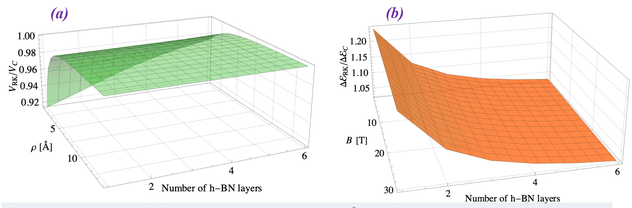

Fig. 4: Adopted from [17]. Plotted for Si type I at $E = 0.3$ *V*/Å. (*a*) The comparison between V_{RK} and V_C. (*b*) Contributions to the binding energy of magnetoexcitons obtained by using V_{RK} and V_C. V_{RK} and V_C converge as number of layers increase, and $\Delta\mathscr{E}$ calculated using V_{RK} and V_C converge as *N* increases.

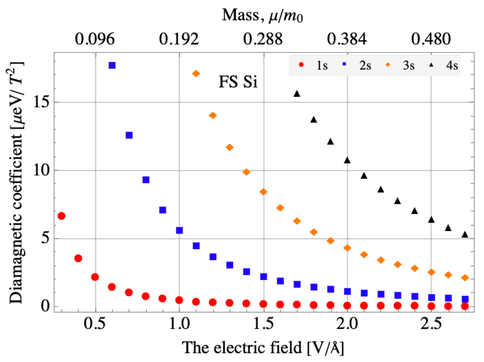

Fig. 5: Adopted from [17]. σ for direct magnetoexcitons in MoS_2 for Rydberg states. σ can be extracted for all four states. Results are published in [17].

Xenes

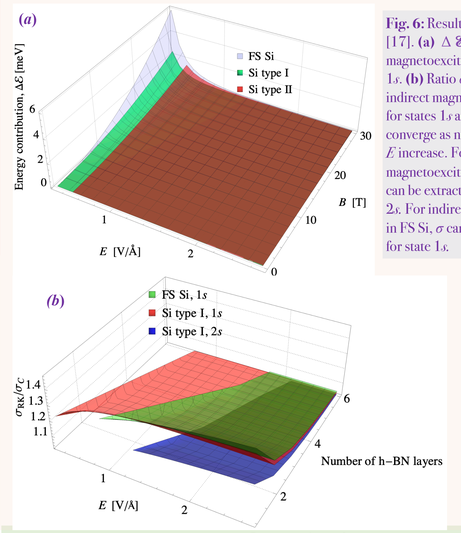

Fig. 6: Results are published in [17]. **(a)** $\Delta\mathscr{E}$ for direct magnetoexcitons in Si in state 1*s*. **(b)** Ratio σ_{RK}/σ_C for indirect magnetoexcitons in Si for states 1*s* and 2*s*. σ_{RK} and σ_C converge as number of layers and *E* increase. For indirect magnetoexcitons in Si type I, σ can be extracted for states 1*s* and 2*s*. For indirect magnetoexcitons in FS Si, σ can be extracted only for state 1*s*.

Conclusion

- In heterostructures, $\Delta\mathscr{E}$ calculated with V_{RK} and V_C converge as *N* and E increase in TMDCs and Xenes.
- σ can be extracted for direct magnetoexcitons in TMDCs for states 1*s* and 2*s*. σ can be extracted for direct magnetoexcitons for state 1*s*.
- σ can be extracted for direct magnetoexcitons in Xenes for states 1*s*, 2*s*, 3*s*, and 4*s*. σ can be extracted for indirect magnetoexcitons for state 1*s*.
- Magnetic field can be used to tune the energy contribution to the binding energy of both direct and indirect magnetoexcitons in TMDCs.
- Electric and magnetic fields can be used to tune the energy contribution to the binding energy of both direct and indirect magnetoexcitons in Xenes.
- We show that it is essential to use correct parameters of materials for calculations.
- By calculating $\mathscr{E}$ with V_{RK} and V_C, we show that it is essential to use appropriate interaction potential to describe interactions between electrons and holes in heterostructures when only few *h*-BN layers separate Xene monolayers.
- TMDCs and Xenes can be used for electronic devices that can be manipulated by electric and magnetic fields.

Acknowledgment

This work is supported by the U.S. Department of Defense under Gran No. W911NF1810433

References: [1] C. Grazianetti, C. Martella, and A. Molle, Phys. Status Solidi RRL 2019, 1900439.
[2]H. Herold, H. Ruder, and G. Wunner, J. Phys. B: At. Mol. Phys. 14, 751 (1981).
[3] N.S. Rytova, Proc. Moscow State University, Phys. Astron. 3, 30 (1967).
[4] L.V. Keldysh, JETP Lett. 29, 658 (1979).
[5] M. N. Brunetti, O. L. Berman and R. Ya. Kezerashvili, IOP Publishing.
[6] R. J. Elliott and R. Loudon, J. Phys. Chem. Solids 15, 196 (1960).
[7] H. Hasegawa and R. E. Howard, J. Phys. Chem. Solids 21, 179 (1961).
[8] L.P.GorKov and I.E. Dzualoshinskii, Zh. Eksp.Teor. Fiz. 53, 717722 (1967).
[9] Yu.E.Lozovick and A.M.Ruvinsky, Phys.Rev. Lett. A.227, 271284 (1997).
[10]S. N. Walck and T. L. Reinecke, Phys. Rev. B 57, 9088 (1998).
[11] M. M. Fogler, L. V. Butov and K. S. Novoselov, Nat Commun 5 4555 (2014)
[12] A. Spiridonova, Phys. Lett. A, 384(33), 126850 (2020).
[13] L. Matthes, O. Pulci, and F. Bechstedt, J. Phys.-Condes. Matter 2013, 25, 395305.
[14] L. Tao, E. Cinquanta, D. Chiappe, C. Grazianetti, M. Fanciulli, M. Dubey, A. Molle, and D. Akinwande, Nat. Nanotechnol. 10, 227-231 (2015).
[15] L. Li, X. Wang, X. Zhao, and M. Zhao, Phys. Lett. A 377(38), 2628-2632 (2013).
[16] Z. Ni, Q. Liu, K. Tang, J. Zheng, J. Zhou, R. Qin, Z. Gao, D. Yu, and J. Lu, Nano Lett. 12, 113-118 (2012).
[17] R. Ya. Kezerashvili and A. Spiridonova, arXiv:2011.03093v1 [cond-mat.mes-hall] .
[18] F. Pan, Y Wang, K. Jiang, Z. Ni, J. Ma, J. Zheng et al., Sci Rep 5, 9075 (2015).